MOLECULAR AND CELLULAR BIOLOGY, Aug. 1995, p. 4031–4042 Vol. 15, No. 8
0270-7306/95/$04.00+0

A Link between Increased Transforming Activity of Lymphoma-Derived *MYC* Mutant Alleles, Their Defective Regulation by p107, and Altered Phosphorylation of the c-Myc Transactivation Domain

ARTHUR T. HOANG,[1] BART LUTTERBACH,[2] BRIAN C. LEWIS,[1] TAKAHIRO YANO,[3]* TEH-YING CHOU,[1] JOHN F. BARRETT,[1] MARK RAFFELD,[3] STEPHEN R. HANN,[2] AND CHI V. DANG[1,4,5]*

Division of Hematology, Department of Medicine,[1] Department of Cell Biology and Anatomy,[4] and The Johns Hopkins Oncology Center,[5] The Johns Hopkins University School of Medicine, Baltimore, Maryland 21205; Department of Cell Biology, Vanderbilt University, Nashville, Tennessee 37232[2]; and Laboratory of Pathology, National Cancer Institute, Bethesda, Maryland 20892[3]

Received 22 November 1994/Returned for modification 18 January 1995/Accepted 2 May 1995

The c-Myc protein is a transcription factor with an N-terminal transcriptional regulatory domain and C-terminal oligomerization and DNA-binding motifs. Previous studies have demonstrated that p107, a protein related to the retinoblastoma protein, binds to the c-Myc transcriptional activation domain and suppresses its activity. We sought to characterize the transforming activity and transcriptional properties of lymphoma-derived mutant *MYC* alleles. Alleles encoding c-Myc proteins with missense mutations in the transcriptional regulatory domain were more potent than wild-type c-Myc in transforming rodent fibroblasts. Although the mutant c-Myc proteins retained their binding to p107 in in vitro and in vivo assays, p107 failed to suppress their transcriptional activation activities. Many of the lymphoma-derived *MYC* alleles contain missense mutations that result in substitution for the threonine at codon 58 or affect sequences flanking this amino acid. We observed that in vivo phosphorylation of Thr-58 was absent in a lymphoma cell line with a mutant *MYC* allele containing a missense mutation flanking codon 58. Our in vitro studies suggest that phosphorylation of Thr-58 in wild-type c-Myc was dependent on cyclin A and required prior phosphorylation of Ser-62 by a p107-cyclin A-CDK complex. In contrast, Thr-58 remained unphosphorylated in two representative mutant c-Myc transactivation domains in vitro. Our studies suggest that missense mutations in *MYC* may be selected for during lymphomagenesis, because the mutant *MYC* proteins have altered functional interactions with p107 protein complexes and fail to be phosphorylated at Thr-58.

The *MYC* proto-oncogene encodes a helix-loop-helix–leucine zipper (HLH-Z) transcription factor that participates in the regulation of cell proliferation, cell differentiation, and apoptosis (13, 17, 18, 21, 43, 58). Deregulation of *MYC* expression appears to be involved in the pathogenesis of a variety of human neoplasms. Two regions of the Myc protein required for its biological activities are the N-terminal transcription activation domain (TAD) and the C-terminal basic-HLH-Z-specific DNA-binding domain (18, 67). The HLH-Z domain mediates dimerization of Myc with its partner, Max, and aligns the adjacent basic regions in the major groove of DNA for recognition of the specific E-box sequence, CAC(A/G)TG (2, 3, 7, 10–13, 17, 29, 44, 46, 50, 57, 58, 69). The TAD of Myc has been shown to activate transcription in the chimeric GAL4 system as well as through E-box sequences with full-length Myc (6, 33, 42, 46, 55, 62, 63). Myc may also interact with TFII-I and impede transcription that is dependent on the initiator (Inr) element (49, 55, 62, 63). Although the Myc TAD has been shown to contact the TATA-binding protein (TBP), the mechanisms by which Myc regulates transcription in normal and neoplastic cells remain poorly understood (36, 52).

* Corresponding author. Mailing address for Chi V. Dang: Ross Research Building, Room 1025, The Johns Hopkins University School of Medicine, 720 Rutland Ave., Baltimore, MD 21205. Phone: (410) 955-2773. Fax: (410) 955-0185. Present address for Takahiro Yano: Thomas Jefferson University, BLSB Room 608, 233 South 10th St., Philadelphia, PA 19107.

Clues to the importance of the Myc N-terminal TAD in neoplastic transformation were recognized through studies of Myc mutants and related TADs of L-Myc and B-Myc (4, 61). L-Myc, which is less potent than c-Myc in transforming fibroblasts, contains a weaker TAD than c-Myc, as determined by using the heterologous yeast GAL4 DNA-binding domain assay. B-Myc is a short protein whose entire length is homologous to the Myc TAD; it does not contain a recognizable DNA-binding motif. B-Myc is capable of squelching c-Myc transactivation and inhibiting c-Myc-mediated transformation. These studies suggest a correlation between Myc transactivation and transforming activities, although there are mutants of Myc that are capable of transactivation but incapable of transformation (42).

Recently, closer examination of Burkitt and AIDS-related lymphomas reveal that in addition to translocated *MYC* alleles, *MYC* exon 2 encoding the TAD is also the target for multiple point mutations (8, 9, 16, 60, 70). These mutations, which are also found in comparable positions in retroviral v-*myc* (54), occur in more than 50% of Burkitt lymphomas and cluster in hot spots involving Glu-39, Thr-58, Ser-62, and Phe-138 (Fig. 1). The high prevalence of these mutations suggests a biological role for these alterations in the genesis of lymphomas. A recent study of three such mutants indicates that the retinoblastoma protein (pRB)-related protein p107 binds to the Myc TAD and inhibits wild-type but not mutant Myc-GAL4 chimeric proteins (5, 32). p107 is a cellular protein that was first identified through its association with simian virus 40 large T

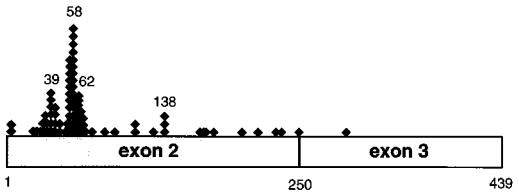

FIG. 1. Frequency of *MYC* coding sequence mutations in v-*myc* and in Burkitt and AIDS-related lymphomas. The bar depicts the c-Myc protein encoded by *MYC* exons 2 and 3. Numbers above and below the bar represent amino acid positions. The number of diamonds (height) above the bar corresponds to the number of mutations at the indicated amino acid position. Hot spots involving Glu-39, Thr-58, Ser-62, and Phe-138 are highlighted by the numbers above the bar. Data were derived from studies of Albert et al. (1), Bhatia et al. (8, 9), Clark et al. (16), Papas and Lautenberg (54), Rabbitts et al. (60), and Yano et al. (70).

antigen and adenovirus E1A protein (22, 26, 35, 71). Similar to pRB p105, p107 causes cellular growth arrest in late G_1 and was found to be associated with the transcription factor E2F (65). Unlike pRB, however, p107 binds directly to cyclins A and E (25, 27, 48) and causes G_1 arrest in a cell line, C33A, which resists pRB-mediated growth arrest (72). The physiological significance of the Myc-p107 interaction remains, however, undetermined. Additionally, the transforming activities of lymphoma-derived Myc mutants and the mechanism of p107-mediated suppression of Myc transactivation remain unknown.

In this report, we demonstrate that a group of lymphoma-derived mutant *MYC* alleles has increased transforming activity unassociated with an attenuated potential to induce apoptosis. These alleles encode mutant Myc proteins that resist p107-mediated suppression of Myc transactivation. These mutations cluster in *MYC* exon 2 hot spots that encode in vivo phosphorylation sites (Thr-58 and Ser-62) in the Myc TAD. Our studies suggest that the resistance of mutant Myc proteins to p107 suppression does not result from the disruption of a physical interaction between Myc and p107. Rather, disruption of a p107-mediated phosphorylation of these Myc mutants may be responsible for their transforming and transactivation properties.

MATERIALS AND METHODS

Plasmid constructions. (i) Myc, p107, and pRB in expression vectors. The wild-type Myc expression vector driven by the Moloney murine leukemia virus long terminal repeat is as described previously (67). Expression vectors containing tumor-derived *MYC* mutations were generated by exchanging the wild-type 414-bp *Pst*I-*Pst*I region in *MYC* exon 2 with the corresponding mutant fragments of cloned PCR-amplified lymphoma DNA (70). Thus, only mutations between amino acids (aa) 41 to 178 are included; mutations excluded are in parentheses in Fig. 2A. Expression of full-length p107 (gift from M. Ewen) is driven by a cytomegalovirus promoter in pCMVneo (24). The simian virus 40 promoter-driven pSG5RB (pRB) expression vector was a gift from W. Kaelin.

(ii) GAL4 fusion and GAL4 reporter constructs. Constructs encoding a chimeric GAL4 DNA-binding domain fused to various TADs are as described previously: GAL4-Myc and GAL4-VP16 (42) and GAL4-NF1 (NF1 aa 220 to 499) (39).

To create chimeric GAL4-mutant *MYC* (designated by B followed by a number [70]) constructs, PCR-amplified *MYC* exon 2 DNA (750 bp) fragments (5′ primer, GCGCGCGC CATATGCCCCTCAACGTTAG; 3′ primer, ACCACC AG CAGCGACTCTTAAGGATCCGCG) containing missense mutations from B3 to B19 alleles were subcloned into pGALM (42) via the *Nde*I and *Bam*HI sites. GAL4-MTA (Thr-58→Ala) was constructed by PCR-assisted site-directed mutagenesis of GAL4 fused to wild-type Myc aa 1 to 262.

To generate the chimeric GAL4-p107 plasmid, a 3-kb *Eag*I-*Pst*I-restricted p107 cDNA fragment (in which the *Eag*I end was blunted by Klenow enzyme fill-in) was subcloned into pGALO (42) between the *Sma* and *Pst*I sites in the polylinker region. The chimeric protein contains p107 aa 34 through 1127.

The GAL4-TBP fusion was constructed by fusing in frame full-length human TBP cDNA (1.5-kb *Nde*I-*Bam*HI fragment) from pT7hTF2D (gift from D. Hawley [66]) to pGALO through compatible *Nde*I-*Bam*HI sites.

pGAL4-RB was constructed by subcloning a 1.6-kb *Eco*RI retinoblastoma gene cDNA fragment (encoding aa 379 to 928) into the *Eco*RI site of pGALO. The retinoblastoma gene cDNA and pE7-VP16 were gifts from W. Kaelin.

GAL4-Myc proteins purified from bacteria were expressed from an expression vector containing hexahistidine-tagged GAL4 sequences (residues 1 to 147) fused to either wild-type or mutant c-Myc sequences. The expression vector pET156-GAL4 was a gift from R. Wisdom. Partially digested *Xho*I-*Bam*HI fragments containing wild-type or mutant GAL4-*MYC* sequences were subcloned into pET156-GAL4 to produce pH6GAL4-Myc, pH6GAL4-MycB3S, and pH6GAL4-MycB19.

The G5E1bCAT reporter construct (gift from J. Lillie and M. Green) (42) and the G5TATALUC and G5InrLUC reporter constructs (gifts from C. Chang and J. Gralla) (15) are as described elsewhere.

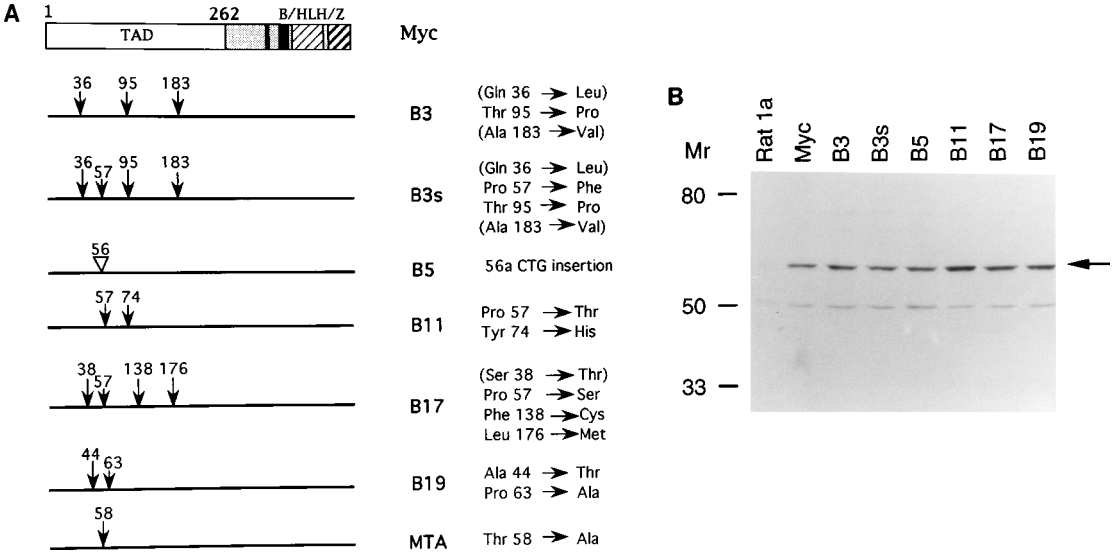

FIG. 2. Expression of wild-type or lymphoma-derived mutant *MYC* in stably transfected Rat 1a fibroblasts. (A) The top bar depicts wild-type Myc, with the TAD and DNA-binding domain (B/HLH/Z) indicated. Sites of missense mutations (arrows) in seven *MYC* alleles derived from six different lymphomas are shown below wild-type Myc. Mutants B3 and B3s are derived from two separate clones from the same tumor. Mutations in parentheses in each case are not included in the full-length Myc expression plasmid (see Materials and Methods). (B) Western blot showing the presence of the 64-kDa human c-Myc protein (arrow) in extracts from equivalent numbers of Rat 1a cells stably transfected with wild-type or mutant Myc (indicated above each lane). Positions (in thousands) of prestained molecular weight markers are indicated on the left.

(iii) *MYC*-VP16 fusion constructs. *MYC*-VP16 was generated by subcloning an 800-bp *Nde*I-*Xba*I *MYC* fragment from GM(1-262) (42) into compatible sites in pNLVP (19, 28). MTA-VP16 was subcloned in a similar manner. To create VP16 fusion constructs containing other lymphoma-derived *MYC* mutations (B3 to B19), fragments containing missense mutations were subcloned from GAL4-B3 through GAL4-B19 via *Sal*I-*Xba*I sites into the pNLVP expression vector.

(iv) Expression plasmids for in vitro transcription and translation. Full-length wild-type *MYC* from pSP64myc (15a) was subcloned downstream of an SP6 promoter into the pGEM-11Zf vector (Promega) via compatible *Eco*RI and *Xba*I sites to create pGEM-11Zf-myc. Fragments containing *MYC* mutations from GAL4-B11, GAL4-B19, and GAL4-MTA were excised via internal *Pst*I-*Pst*I restriction sites (aa 41 to 178) and subcloned into the corresponding sites in wild-type *MYC* (pGEM-11Zf-myc). The *MYC* deletion mutant D41-178 was generated by removal of the internal *Pst*I-*Pst*I fragment and religation. *MYC* deletion D1-100 has been described elsewhere (51).

Expression and purification of GST-p107 and GST-myc100 fusion protein. GST-p107 was constructed by subcloning the ~3-kb *Eco*RI-*Pst*I (blunt ended with Klenow enzyme) fragment from GAL4-p107 into compatible *Eco*RI-*Sma*I sites of pGEX1 (Pharmacia). The GST-p107 fusion protein was produced in transformed *Escherichia coli* JM89 by isopropylthiogalactopyranoside (IPTG) induction for 4 h prior to purification as described elsewhere (41). Briefly, after IPTG induction, JM89 grown in 1 liter of LB broth was spun down and resuspended in 10 ml of phosphate-buffered saline (PBS), sonicated for 30 s, and then solubilized with 1% (vol/vol) Triton X-100. Following centrifugation, the supernatant was incubated with 2 ml of a 50% slurry of GS-Sephacyl beads (Pharmacia) for 10 min at room temperature. The beads were then washed thrice with 50 ml of cold PBS and resuspended into 1.25 ml of PBS. GST-myc100 was constructed and purified as described previously (51).

Expression and purification of GAL4-Myc fusion proteins. *E. coli* B3CL was transformed with pH6GAL4-Myc plasmids and induced to express the proteins with IPTG. Bacterial lysates were denatured in 6 M guanidinium-HCl, and the His-tagged proteins were purified as previously described (44).

In vitro Myc-p107 binding assay. Myc proteins were produced by coupled in vitro transcription and translation in rabbit reticulocyte lysate reactions as described by Promega. DNA template (1 μg) was added to transcription-translation lysate (50 μl) containing 40 μCi of [^{35}S]methionine, and the mixture was incubated at 30°C for 2 h. ^{35}S-labeled product (4% of the total) was suspended into 20 μl of 2× Laemmli buffer, heated, and then electrophoresed (10% sodium dodecyl sulfate [SDS]-polyacrylamide gel). The resultant gel was fixed, treated with Amplify (Amersham), dried, and exposed to Hyperfilm at −70°C for 14 h.

To determine *MYC* interaction with GST-p107 in vitro, an aliquot (4% of total lysate described above) of programmed lysate was added to 50 μl of either GST or GST-p107 beads equilibrated with kinase reaction buffer (KB; 50 mM *N*-2-hydroxyethylpiperazine-*N*′-2-ethanesulfonic acid [HEPES; pH 7.3], 10 mM $MgCl_2$, 3 mM $MnCl_2$, 1 mM dithiothreitol, 20 mM β-glycerophosphate). Following 1 h of incubation at 4°C, the beads were washed thrice with NETN buffer (0.5% Nonidet P-40, 20 mM Tris-HCl [pH 8], 0.1 M NaCl, 1 mM EDTA), resuspended in 20 μl of 2× Laemmli buffer, and heated prior to SDS-polyacrylamide gel electrophoresis (PAGE) analysis.

Western blotting (immunoblotting) and immunoprecipitation. For Western blot analysis, total cell lysates collected from plates of exponentially growing cells at 70% density were boiled in 2× Laemmli buffer (47). Polypeptides from 1/10 of total cell lysates from each plate (100 by 20 mm) were resolved by SDS-PAGE (10% gel) and subjected to immunoblot analysis using rabbit anti-Myc polyclonal antibody MC1 (1:5,000 dilution) (gift from P. Devreotes). This antibody was generated against a human C-terminal Myc sequence. Detection was achieved with a secondary goat anti-rabbit horseradish peroxidase-conjugated antibody (1:10,000 dilution) (Bio-Rad) and enhanced chemiluminescence (Amersham).

Chinese hamster ovary (CHO) cells transiently transfected with 4 μg of the different GAL4 fusion constructs per 100-mm-diameter plate were metabolically labeled 48 h posttransfection with [^{35}S]methionine for 4 h. Immunoprecipitation was performed with a rabbit polyclonal anti-GAL4 antibody (gift of I. Sadowski) as described previously (44).

Cell lines. Rat 1a fibroblasts carrying wild-type or mutant *MYC* were generated by cotransfection (Lipofectin; Bethesda Research Laboratories) with the different Moloney murine leukemia virus long terminal repeat-driven genomic *MYC* alleles (B3 through B19) (10 μg of DNA per 100-mm-diameter plate) and a neomycin resistance marker plasmid (pSV2neo) (1 μg of DNA per 100-mm-diameter plate). Cells were selected with the antibiotic G418 (400 μg of active G418 per ml in Dulbecco's minimal essential medium [DMEM] with 10% fetal calf serum). More than 100 G418-resistant clones from each separate transfection were pooled for subsequent analyses.

Soft agar growth assay. For the soft agarose transformation assay, 10^5 cells in twofold-concentrated DMEM and 20% fetal calf serum were mixed with an equal volume of 0.8% agarose (45°C) (SeaKem) and poured onto a bed of 1.4% agarose (SeaKem). The plates were fed every 3 days with 2 ml of DMEM containing 10% fetal calf serum. At 14 days after plating, photomicrographs of colonies were obtained. Photographs of various microscopic fields were enlarged, and the diameters of all colonies within the fields were measured. For each pooled cell line, at least 160 colonies were measured, and colony sizes are shown as normalized histograms.

Transient transfection and CAT assay. To determine the effect of p107 on GAL4-*MYC* or GAL4-*MYC* mutants, CHO cells in 100-mm-diameter plates were transiently transfected by using DEAE-dextran as described previously (42). The amounts of plasmid DNA transfected per 100-mm-diameter plate were 2 μg of reporter chloramphenicol acetyltransferase (CAT) construct, 1 μg of GAL4 fusion, and 3 μg of p107 or pRB expression plasmid. CAT assays were performed as described previously (42), and CAT activities were normalized to the amount of cellular protein (Bradford assay; Bio-Rad) recovered.

Mammalian two-hybrid assay. Determination of *MYC*-p107 interaction in vivo was performed by transient transfection using CHO cells (19, 28). The amounts of plasmid DNA used per 100-mm-diameter plate were 1 μg of CAT or luciferase reporter, 1 μg of GAL4-p107 or GAL4-TBP, and 2 μg of wild-type or mutant *MYC*-VP16 expression plasmid. Luciferase activity was determined by using a Promega assay kit. CAT and luciferase activities were corrected for total amounts of cellular protein recovered.

In vitro phosphorylation assay. c-Myc chimeric or full-length proteins were subjected to phosphorylation reactions using three different experimental designs. In the first design, immobilized glutathione *S*-transferase (GST)–p107 or GST alone was incubated with reticulocyte lysate programmed with pSP6-cyclin A (kindly provided by T. Hunter and J. Pines) (56) or control lysate to form a p107-cyclin A-CDK complex. Purified Myc protein was then incubated with the immobilized complex or control in KB as described by Lutterbach and Hann (51). The Sephadex-GST-p107 or GST-alone beads were washed thrice with KB, and the resultant material was analyzed by SDS-PAGE.

In the second protocol, Myc proteins were incubated with control lysate or reticulocyte lysate programmed with cyclin A in KB for 30 min. The resultant products were incubated with Sephadex-GST-p107 to recover Myc protein. The bound material was separated on an SDS-polyacrylamide gel, and phosphorylated Myc proteins were subjected to phosphopeptide analysis.

In the third design, an equal volume of a 50% Sephacyl slurry containing either GST-p107 or GST alone was incubated (1 h at 4°C) with rabbit reticulocyte transcription-translation lysate (50 μl) programmed with or without cyclin A. After incubation, the slurry was washed thrice with NETN buffer, and the GST-p107-cyclin A-CDK complex was eluted from Sephadex beads by addition of 5 mM reduced glutathione (pH 7.5). An in vitro phosphorylation assay was then performed in 25 μl of 1× KB with or without GST-myc100 (1 μg) and 10 μCi of [γ-^{32}P]ATP. The resultant product was suspended in 2× Laemmli buffer, boiled, and subject to SDS-PAGE (10% gel) analysis.

Phosphopeptide mapping. To determine the in vivo phosphorylation status of Myc, approximately 5×10^7 cells were metabolically labeled with 12.5 μCi of $^{32}P_i$ (ICN, Costa Mesa, Calif.) for 2 h at 37°C in phosphate-free medium. Cellular lysates were then prepared, and the Myc proteins were immunoprecipitated as described previously (51). Briefly, labeled cells were washed twice with 10 mM Tris-HCl (pH 8)–150 mM NaCl and lysed in cold antibody lysis buffer (51) containing 10 mM iodoacetamide, 50 mM NaF, and 0.1 mM Na_3VO_4. Lysates were then sonicated and precleared with *Staphylococcus aureus* membranes (Immuno-Precipitin; Bethesda Research Laboratories), and the Myc proteins were immunoprecipitated with 5 μg of affinity-purified anti-Myc peptide antibody or 5 μl of anti-GST-myc100 serum and Immuno-Precipitin. Samples were subjected to SDS-PAGE (10% gel) and transferred to nitrocellulose. The phosphorylated Myc proteins were then digested with proteases, and phosphopeptides were processed as described previously (14). The recovered phosphopeptides were subjected to electrophoresis in a Hunter thin-layer electrophoresis chamber in pH 1.9 buffer (1.5 kV, 20 min) and ascending chromatography in phosphochromatography buffer (14). Autoradiography of electrophoretic plates was performed as described elsewhere (51).

RESULTS

Lymphoma-derived Myc mutants have increased transforming activity. The prevalence of *MYC* exon 2 mutations in Burkitt lymphomas and tumor-derived cell lines, and comparable mutations in v-Myc, suggests that these mutations may provide a growth advantage for cells containing them (8, 9, 16, 60, 70). The growth advantage conferred by *MYC* missense mutations may result from enhanced *MYC*-induced cellular proliferation or may result from attenuation of Myc-mediated apoptosis (23, 67). To test these hypotheses, we isolated mutated sequences from six translocated Burkitt lymphoma *MYC* alleles by PCR (Fig. 2A) (70). *Pst*I-restricted exon 2 DNA fragments were subcloned into Myc expression vectors to produce Myc proteins containing mutations around Thr-58 (between aa 41 and 178).

For transformation assays, we chose Rat 1a fibroblasts, which show anchorage-independent growth in the presence of overexpressed *MYC* alone (67), in contrast to primary fibroblasts, which require both *MYC* and an activated *RAS* gene.

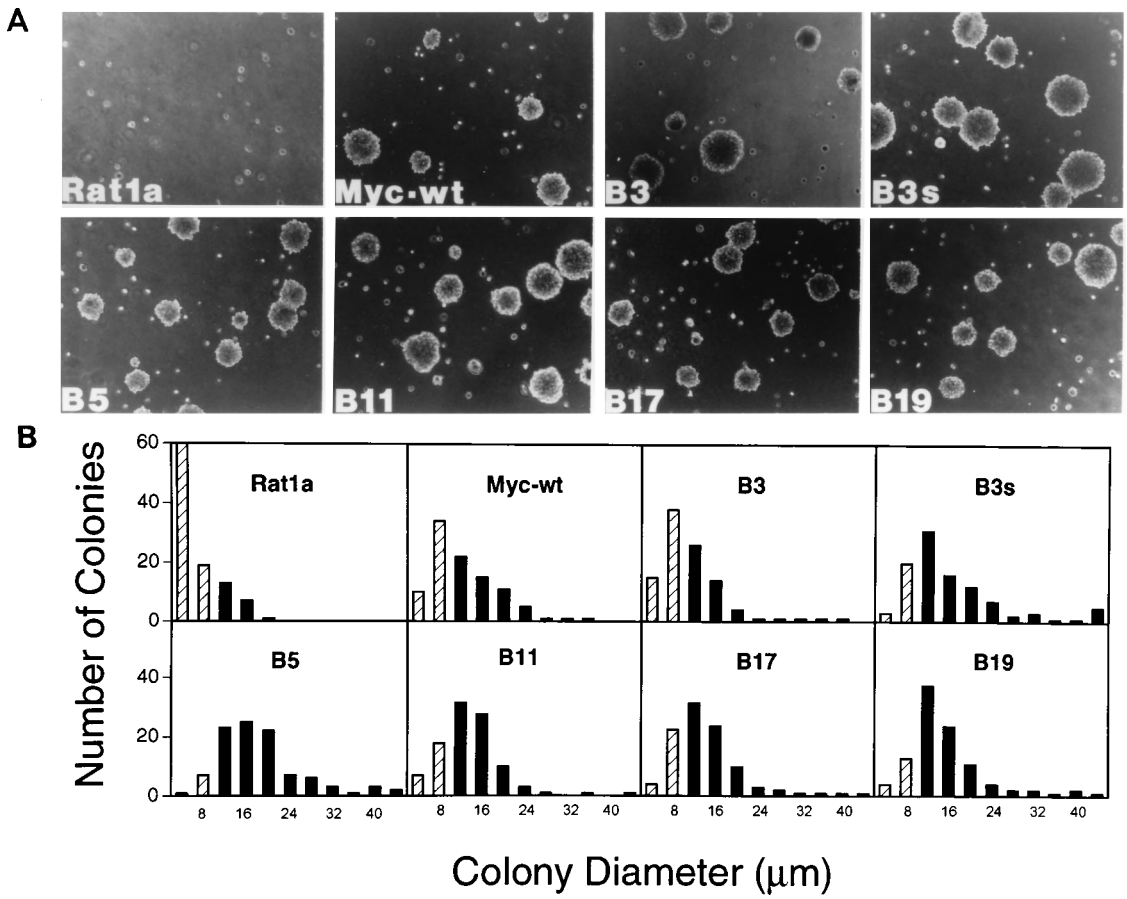

FIG. 3. Transformation of Rat 1a fibroblasts stably transfected with wild-type or mutant *MYC* alleles. Representative phase-contrast photomicrographs of Rat 1a colonies expressing wild-type Myc (Myc-wt) or mutant Myc were taken 16 days after plating in soft agarose (A). Shown below for each pooled cell line are histograms representing the distribution of colony sizes obtained at 8 days after plating. For each pooled cell line, colony sizes from at least 160 colonies were measured from duplicate experiments and normalized to the value for 100 colonies (B). Striped bars represent colony sizes frequently found in the parental Rat 1a mocked-transfected cell line; filled bars represent large colonies.

This choice avoids the confounding factor contributed by *RAS* and allows measurement of Myc protein levels in stably transfected Rat 1a cells. Our choice of the Rat 1a cell transformation assay further allows us to assess Myc-induced apoptosis, which does not occur in primary cells transformed by both *MYC* and activated *RAS*. Therefore, Rat 1a fibroblasts were stably transfected with mutant or wild-type *MYC* alleles. The levels of Myc proteins in stably transfected Rat 1a cells were comparable, as determined by immunoblot analysis using an antibody specific for human c-Myc protein (Fig. 2B).

To determine the transforming potential of the mutant *MYC* alleles, anchorage-independent growth properties of pooled Rat 1a cell lines expressing mutant Myc proteins were compared with those of a cell line expressing the wild-type protein (Fig. 3A). Expression of these mutant *MYC* alleles, except B3, resulted in enhanced transformation of Rat 1a cells, as evidenced by an increase in the number of large colonies (Fig. 3B). The mutant alleles caused an increase in the formation of colonies that were 12 μm or greater in diameter compared with colonies containing wild-type MYC at 8 days in culture. The increases were as follows: B3S, 32%; B5, 62%; B11, 32%; B17, 31%; and B19, 51%. The anchorage-independent growth assays were performed in duplicate and yielded similar results in three separate experiments. It is notable that the most prevalent coding sequence alteration of *MYC* (Fig. 1) in Burkitt lymphomas, AIDS-related lymphomas (8, 9, 16, 60, 70), and three separate *myc* transducing retroviruses (54) involves Thr-58 (mutant MTA in Fig. 2). Mutations affecting this residue have been previously shown to augment c-Myc transforming activity (37, 59). Thus, mutations affecting or flanking Thr-58 result in enhanced Myc transforming potential.

Since augmented transforming activities of mutant *MYC* alleles may result from an increase in the rate of cellular proliferation or decrease in Myc-induced apoptosis, we determined whether the mutations attenuate Myc-induced apoptosis, thereby increasing Myc transforming activity. This issue is particularly important as we have observed cell death in the center of colonies of Myc-expressing Rat 1a cells in agarose but not in cells expressing both Myc and Bcl-2 (38, 38a). When serum was withdrawn, the extent of Myc-induced apoptosis was not attenuated by mutant *MYC* alleles compared with wild-type *MYC* (data not shown) (23). At 24 h after serum withdrawal, deregulated expression of wild-type or mutant *MYC* alleles induces death in 20 to 30% of the cells, as determined by trypan blue dye exclusion or in situ end labeling of nicked DNA (31) (data not shown). These observations suggest that mutant *MYC* alleles derived from lymphomas have an increased transforming capability without loss of the ability to induce apoptosis.

Selective suppression of Myc transactivation by p107. The majority of the tumor-derived *MYC* mutations are present

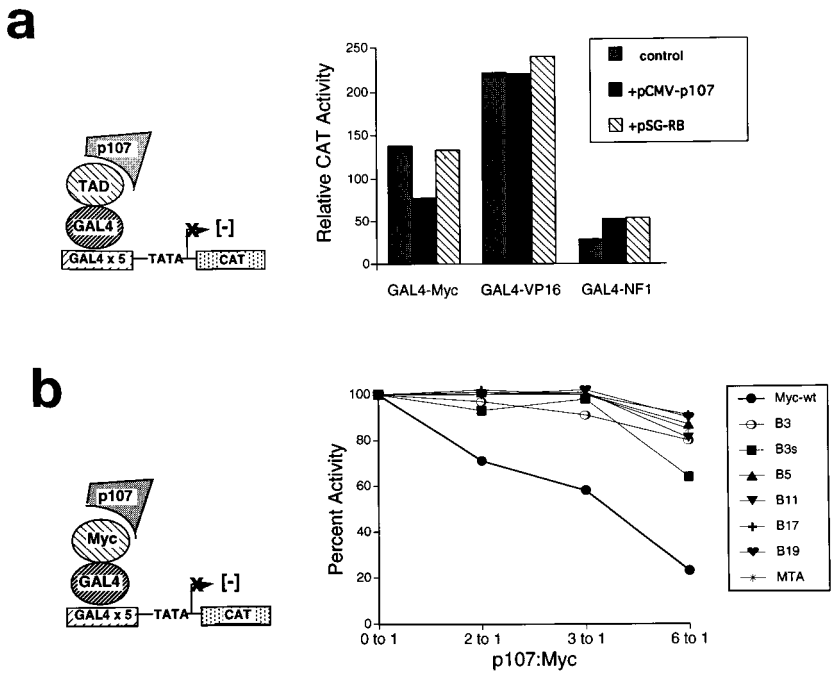

FIG. 4. Selective suppression of Myc transactivation by the pRB-related protein p107. (a) The schematic drawing depicts suppression of TADs by p107. The reporter CAT construct contains five GAL4 binding sites upstream of an adenoviral E1b TATA box. Bar graphs show relative reporter activities resulting from duplicate experiments with chimeric GAL4 proteins containing Myc, acidic VP16, or proline-rich NF1 TADs in the presence of p107 (black bars) or pRB (striped bars). The weight ratios of p107 or pRB expression plasmids to those of GAL4 chimeras were 3:1. Control (gray) bars denote reporter CAT activity in the presence of the individual GAL4-TAD fusion constructs. (b) Effect of p107 on the activities of GAL4 chimeric proteins containing wild-type Myc (Myc-wt) or mutant Myc transactivation domains. The schematic drawing is similar to that in panel a. The percent activity of each chimeric GAL4 protein with increasing amounts of p107 expression plasmid is shown. Each datum point is an average from four experiments. Errors were less than 10% of the reported value.

within the Myc N-terminal TAD that was originally identified through studies of GAL4-Myc chimeric proteins (42). Recently, Gu et al. (32) reported that a labeled c-Myc N-terminal protein fragment interacted with the pRB-related protein p107. Furthermore, studies by Beijersbergen et al. (5) demonstrated that p107 interacts with the Myc TAD both in vitro and in vivo. A consequence of this interaction is suppressed Myc-mediated transactivation.

Since the previous study by Gu et al. (32) compared Myc only with a very potent transactivator, VP16, that may resist suppression by p107 by virtue of its potency, we studied the transactivation domains of Myc, the herpes simplex virus VP16 protein, and the NF1 (CTF1) transactivator (39, 53). Figure 4a shows that both the potent VP16 acidic transactivation domain and the weaker NF1 proline-rich domain were unaffected by p107, whereas the Myc domain was inhibited. Moreover, p107 also failed to inhibit the transactivation domain of USF, a Myc-related HLH-Z protein that has the same *MYC* consensus binding site (21a). In contrast to p107, an expression vector for pRB, did not inhibit any of the chimeric GAL4 activators (Fig. 4a) but is capable of inhibiting GAL4-E2F (data not shown) as previously reported (5, 30, 32). These results suggest that p107 selectively inhibited Myc-mediated transactivation.

Mutant Myc TADs resist suppression by p107. The various mutant c-Myc TADs tethered to the GAL4 DNA-binding domains did not display activities that have a consistent pattern of change compared with the wild-type c-Myc TAD. The relative activities of the GAL4-Myc chimeric proteins (in relative light units [mean ± standard deviation] from quadruplicate experiments using 1 μg of activator plasmid) were as follows: wild type, 105,754 ± 19,787 (100%); B3, 158,423 ± 10,147 (149%); B3S, 175,567 ± 12,976 (166%); B5, 95,364 ± 13,015 (90%); B11, 97,814 ± 22,423 (92%); B17, 174,737 ± 60,773 (165%); B19, 105,715 ± 2,998 (99.9%); and MTA, 158,346 ± 28,689 (150%). Because an altered pattern of basal transcriptional activities of chimeric GAL4-Myc proteins was not apparent, we sought to determine whether there is a differential suppression of Myc-mediated transactivation by p107 as previously reported for three Myc mutants (32). Mutant Myc TADs fused to GAL4 (42) were expressed from chimeric GAL4 expression vectors and tested for susceptibility to inhibition by p107. All chimeric proteins were expressed comparably in transiently transfected CHO cells, as determined by immunoprecipitations with an anti-GAL4 antibody (data not shown). By titrating with increasing amounts of p107 expression plasmid, wild-type Myc transactivation was suppressed by p107, whereas transactivation activities of all seven mutants were relatively resistant to suppression by p107 (Fig. 4b). These results confirm and extend the previously reported observation that lymphoma-derived mutant Myc proteins resist suppression of transactivation by p107 (32). It is notable, however, that all mutants studied to date except mutant B3 have alterations around Thr-58.

Mutant Myc TADs do not have decreased binding to p107 or increased binding to TBP. The resistance of mutant Myc to p107-mediated suppression suggests at least two possible and readily testable mechanisms of altered interaction. Mutations in the Myc transactivation domain may directly abrogate the interaction of Myc with p107. Alternatively, since TBP has been demonstrated to interact with the Myc TAD in vitro and perhaps also in vivo (36, 52), the mutations may increase the affinity of the interaction between the Myc TAD and TBP. Such increases in the binding of Myc mutants to TBP may

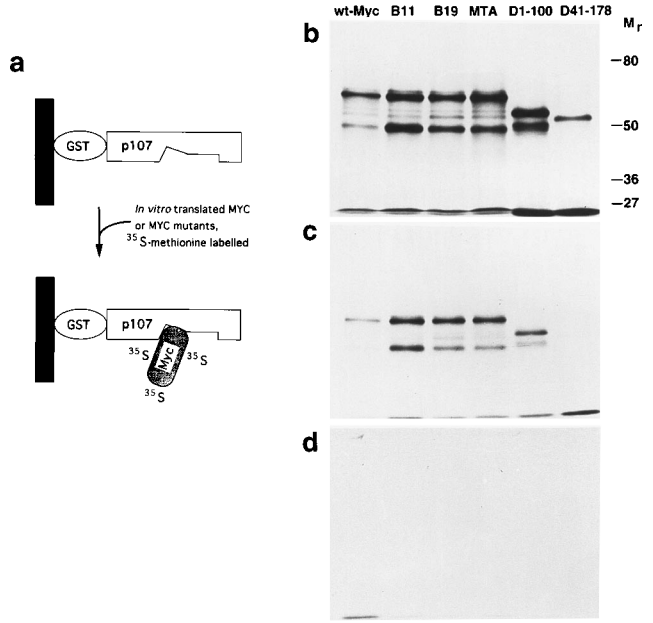

FIG. 5. In vitro interaction between Myc and GST-p107. (a) Diagram depicting the assay for interaction between Myc and GST-p107 immobilized on Sephadex beads. (b) Autoradiogram of an SDS-polyacrylamide gel of wild-type Myc (Myc-wt) or mutant Myc products derived from [^{35}S]methionine-labeled in vitro transcription-translation reactions. The D1-100 mutant has an N-terminal deletion from aa 1 to 100. The D41-178 mutant represents an internal deletion from aa 41 to 178. Positions (in thousands) of molecular weight markers are shown at the right. (c) Autoradiogram of Myc proteins bound to GST-p107. The amount of bound protein was 4 to 10% of total input material (b) as determined from two separate binding assays. (d) Autoradiogram of Myc proteins bound to control GST-Sephadex. The amounts of proteins were identical to those incubated with GST-p107 (c), and the Sephadex beads were washed identically. Autoradiographic and photographic exposure times were identical for experiments with GST-p107 (c) and GST (d).

thereby sterically preclude the access of p107 to mutant Myc TADs.

We examined first the in vitro interaction between p107 and wild-type or mutant Myc proteins. Myc proteins were expressed by in vitro coupled transcription and translation and then subjected to a binding assay using an immobilized GST-p107 fusion protein (Fig. 5a). Figure 5b represents an autoradiogram of [^{35}S]methionine-labeled Myc polypeptides separated by SDS-PAGE. Note that the full-length Myc polypeptides (wild-type Myc, B11, B19, and MTA) migrate with apparent molecular weights of 64,000, whereas prematurely terminated polypeptides migrate at about 45,000 in each lane. While binding of Myc proteins was virtually undetectable with immobilized GST alone (Fig. 5d), we found that the binding of Myc mutants to p107 was similar to that observed with wild-type Myc (Fig. 5c). In addition, deletion of almost the entire Myc TAD (aa 41 to 178; D41-178 in Fig. 5b and c) resulted in loss of p107 binding, whereas removal of the first 100 aa (D1-100 in Fig. 5b) did not abrogate binding. These results suggest that residues 100 to 178 may be important for p107 binding. They contrast, however, with the finding by Gu et al. (32) that transactivation by GAL4 fused to Myc residues 1 to 100 is suppressible by p107, an observation which we are not able to verify (data not shown).

To substantiate the in vitro studies, we further determined the interaction of p107 with either wild-type or mutant Myc TADs in vivo, using a mammalian two-hybrid system (19, 28). In this system, chimeric GAL4-p107 and Myc-VP16 proteins interact to reconstitute a competent GAL4 transactivator that activates a GAL4-dependent reporter construct (Fig. 6a). Whereas an interaction of the wild-type Myc TAD with p107 in the two-hybrid system is detectable (compare bar H with bars A, B, and C in Fig. 6a), an interaction between Myc and pRB (bar G) was undetectable. In control experiments, both GAL4-pRB and GAL4-p107 chimeric proteins interact very effectively with the papillomavirus E7 protein fused to VP16 (bars F, P, and Q). Moreover, in control studies, GAL4-p107 did not interact with either the VP16 TAD alone or the Fos leucine zipper fused to VP16 (bars D and E) (19). As observed in vitro (Fig. 5), mutant Myc TADs interacted with p107 as well as or better than wild-type Myc in the two-hybrid system (bars H through O). These observations are consistent with the results of previously reported immunoprecipitation experiments using three Burkitt lymphoma cell lines (32). In those experiments, the wild-type and all three MYC mutant proteins associated comparably with p107 in cell extracts. Taken together, these findings indicate that these Myc mutations do not disrupt the physical interaction between Myc and p107.

We tested the possibility that tumor-derived Myc mutations enhance an interaction between TBP and the Myc TAD. Such enhanced interaction may cause steric hindrance that accounts for the resistance of the mutant Myc TADs to suppression by p107. An expression vector producing GAL4 fused to full-length human TBP (Fig. 6b) was constructed. To demonstrate the interaction between the Myc TAD and TBP in a two-hybrid system, we used a luciferase reporter driven by upstream GAL4 binding sites and an Inr element (15). The Inr element was chosen to avoid any potential direct interaction of the chimeric GAL4-TBP protein with TATA elements. Although GAL4-TBP yielded significant transactivation of the Inr-driven reporter above the background level (compare bars A and C in Fig. 6b), an interaction with the Myc TAD fused to VP16 was readily detectable (bars B, D, and F). Control experiments with either the expression vector producing the VP16 domain alone or VP16 fused to the Fos leucine zipper (Fos-VP16) indicated no detectable interaction of VP16 or Fos-VP16 with TBP (bars D and E). Although these experiments provided evidence for a specific interaction between the Myc TAD and TBP in vivo, the lymphoma-derived Myc mutations in the context of chimeric GAL4 proteins did not augment the interaction with TBP (bars F through M). These experiments indicate that enhanced interactions between Myc mutants and TBP neither occur nor account for the resistance of these mutants to p107 suppression.

Lack of Thr-58 phosphorylation in a lymphoma-derived mutant Myc in vivo. Given that the resistance of Myc mutants to p107 suppression cannot be explained simply by disruption of a physical interaction between Myc and p107 or by altered interaction of Myc with TBP, we sought to determine whether altered phosphorylation of Myc was associated with the escape from p107 regulation. In support of this hypothesis is the high prevalence of mutations altering Myc (Fig. 1) at two major Myc phosphorylation sites, Thr-58 and Ser-62, in Burkitt and AIDS-related lymphomas (37, 51, 59). In addition, many of the lymphoma-derived Myc mutants contain alterations of amino acids surrounding Thr-58, but in these instances Thr-58 remains unaltered.

We hypothesize that such mutations flanking Thr-58 also affect its in vivo phosphorylation status. Thus, the in vivo phosphorylation maps of wild-type and two Burkitt lymphoma mutants were examined. Since only two Burkitt lymphoma cell lines that are relevant to the mutant *MYC* alleles considered in our study are available, our analysis was limited to these mutants. As a control, the Jurkat T-cell line was used to examine

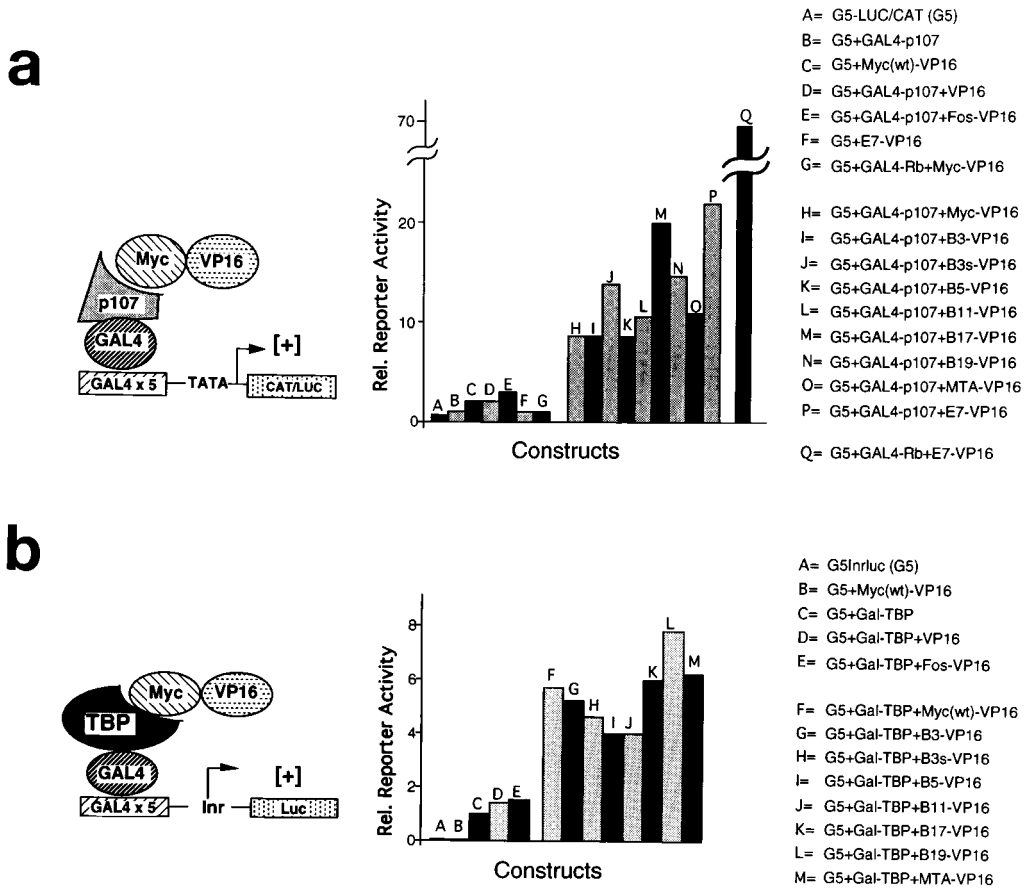

FIG. 6. In vivo interaction between Myc and p107 or TBP as determined by the two-hybrid assay. (a) The diagram depicts the chimeric proteins GAL4-p107 and Myc TAD-VP16 interacting to transactivate the reporter G5E1bCAT or G5TATALUC (luciferase [Luc]) construct. The bar graph represents relative reporter activities resulting from the cotransfection of the reporter with chimeric plasmids defined in the figure. The notation G5 represents the reporter construct. Controls (A to G) are grouped. All values averaged from triplicate experiments are normalized to the GAL4-p107 activity, which is arbitrarily defined as unit activity. Errors were less than 10% of the reported value. (b) The diagram depicts the chimeric proteins GAL4-TBP and Myc TAD-VP16 interacting to transactivate the reporter G5Inr-luciferase construct. The bar graph represents relative reporter activities as shown in panel a. Controls (A to E) are grouped. All values averaged from duplicate experiments are normalized to the GAL4-TBP activity, which is arbitrarily defined as unit activity. Errors were less than 10% of the reported value. Myc(wt), wild-type Myc.

the phosphorylation of wild-type Myc. One of the mutants, B3CL (known as ST486; courtesy of I. Magrath), corresponds to the Myc mutant B3S (Gln-36→Leu, Pro-57→Phe, Thr-95→Pro, Ala-183→Val) that has been shown to have increased transforming activity and resist p107 suppression (Fig. 2). The other cell line, B7CL (known as DW6), was also studied because its mutations (Val-5→Ile, Thr-95→Ala, Phe-115→Leu) are relatively distant from Thr-58. The B7CL Myc mutant notably does not resist p107 suppression of Myc-mediated transactivation (69a). As evident from the phosphopeptide maps (Fig. 7), phosphopeptide b containing phospho-Thr-58 is absent from the B3CL map, suggesting that a mutation adjacent to Thr-58 alter the phosphorylation of this residue in vivo. In contrast, Myc derived from B7CL retains phosphorylation of Thr-58. These observations suggest the hypothesis that alteration of phosphorylation of Myc, perhaps mediated through its interaction with p107, is associated with the resistance of certain lymphoma-derived Myc mutants to suppression by p107.

p107- and cyclin A-dependent in vitro phosphorylation of Myc at Thr-58 and Ser-62. From observations presented above, we hypothesize that p107-mediated phosphorylation of Myc inhibits the function of Myc. We examined the ability of p107-cyclin-CDK complexes to phosphorylate Myc in vitro, specifically since p107 has been found to be associated with either cyclin A or cyclin E (48). To determine whether a p107-cyclin-CDK complex could phosphorylate the Myc N-terminal TAD in vitro, a GST-p107 fusion protein was produced and affinity purified on glutathione-Sepharose beads. In vitro-translated cyclin A and its associated kinase present in rabbit reticulocyte lysate were allowed to bind with immobilized GST-p107. The resultant GST-p107-cyclin A-CDK complexes were subsequently eluted from the beads with glutathione. These cyclin A-dependent kinase complexes were able to mediate the phosphorylation at Ser-62 of a purified GST-Myc fusion protein (51) containing the Myc amino-terminal domain (peptide c in Fig. 8). Some as yet unidentified cyclin A-dependent phosphopeptides migrating anodic to the origin were also observed (data not shown). Note that identification of all in vitro phosphorylation sites was verified by comigration of the in vitro-generated phosphopeptides with those derived in vivo as previously described (data not shown) (51). This in vitro phosphorylation of c-Myc Ser-62 by a p107-cyclin A-dependent kinase is consistent with the previously reported in vitro phosphorylation pattern of this GST-Myc fusion protein with cdc2 kinase alone (51).

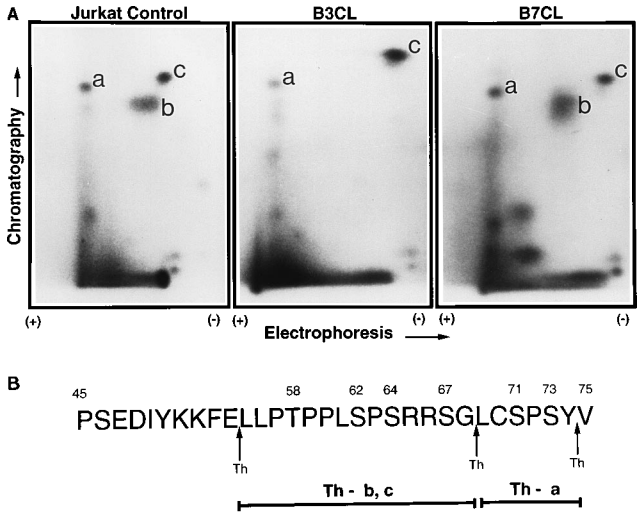

FIG. 7. (A) Phosphopeptide map of c-Myc from wild-type Myc (Jurkat control) and two Burkitt lymphoma cell lines (B3CL and B7CL). B3CL contains mutations at positions 8 (T→S), 36 (Q→L), 57 (P→T), 95 (T→P), and 183 (A→V); B7CL is mutated at positions 5 (V→I), 95 (T→A), 115 (F→L), and 249 (S→G). Two-dimensional electrophoresis and chromatography were performed on thymolysin (Th)-digested c-Myc products previously in vivo labeled with $^{32}P_i$ and purified by immunoprecipitation. (B) Identities and positions of three phosphopeptides, a, b, and c, along with the wild-type c-Myc peptide sequence from aa 45 to 75. Phosphopeptide a is singly phosphorylated at Ser-71. Phosphopeptide c is singly phosphorylated at Ser-62, and phosphopeptide b is doubly phosphorylated at Thr-58 and Ser-62.

Because phosphorylation of Myc Thr-58 has been reported to be dependent on the prior phosphorylation of Ser-62 (51, 59), we determined whether phosphorylation of both Ser-62 and Thr-58 could occur in a cyclin A-dependent fashion in reticulocyte lysate. We used full-length bacterially synthesized Myc lacking the HLH domain as a substrate, since deletion of the HLH domain appears to yield a product that is more soluble than wild-type Myc (20). We observed that the full-length Myc protein could be phosphorylated in a p107- and cyclin A-dependent fashion in vitro in the absence of reticulocyte lysate (Fig. 9). This purified Myc protein was incubated with reticulocyte lysates that were either mocked programmed or programmed with cyclin A transcripts. Although the extents of c-Myc protein phosphorylation with rabbit reticulocyte lysate appear similar in the presence and absence of cyclin A (Fig. 10A), the sites of Myc phosphorylation were dramatically different. By phosphopeptide mapping, we found that in vitro phosphorylation of the Myc transactivation domain residues Thr-58, Ser-62, and Ser-71 has an absolute requirement for cyclin A (Fig. 10B). These Myc residues, which are found phosphorylated in vivo (51), remained unphosphorylated by rabbit reticulocyte lysate in the absence of cyclin A. We have observed variability in the ascending chromatographic migration of c-Myc phosphopeptides generated in vitro. Therefore,

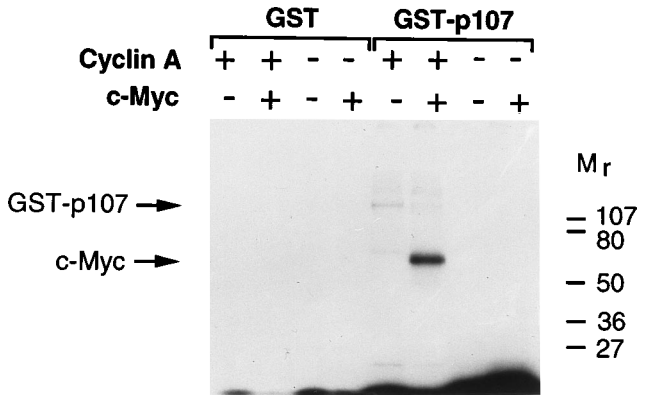

FIG. 9. p107- and cyclin A-dependent phosphorylation of c-Myc in vitro. An autoradiogram of phosphorylation products after separation by SDS-PAGE is shown. Purified human Myc protein produced in bacteria was incubated with either immobilized GST or GST-p107 preloaded with either unprogrammed reticulocyte lysate (−) or lysate containing in vitro-translated human cyclin A (+) as indicated at the top. Alternating lanes represent phosphorylation reactions in the absence (−) or presence (+) of Myc protein. Note that in the absence of c-Myc, cyclin A mediates a detectable autophosphorylation of GST-p107. c-Myc was phosphorylated and bound to the GST-p107 only when both p107 and cyclin A were present. M_r values are indicated in thousands.

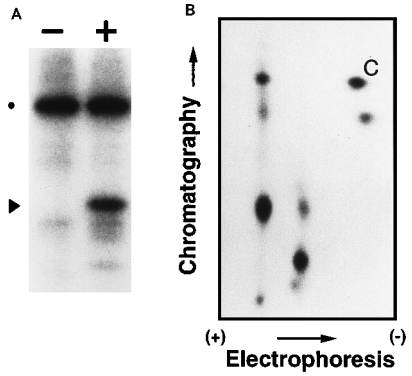

FIG. 8. In vitro phosphorylation reaction of Myc with purified GST-p107 and cyclin A-CDK complexes. (A) Autoradiogram of an SDS-polyacrylamide gel of GST-myc100 (fusion protein of GST and the first 100 N-terminal residues of Myc) phosphorylated by purified p107-cyclin A-CDK complex (arrowhead). Above each lane, + or − denotes the inclusion or exclusion of GST-myc100 in the kinase reaction. The dot denotes the position of autophosphorylated GST-p107 (M_r, ~120,000). (B) Phosphopeptide map of phosphorylated GST-myc100 product purified by SDS-PAGE and subjected to thymolysin digestion as for Fig. 7. The position of phosphopeptide c is marked. Additional unidentified phosphopeptides are also evident close to the origin of the map.

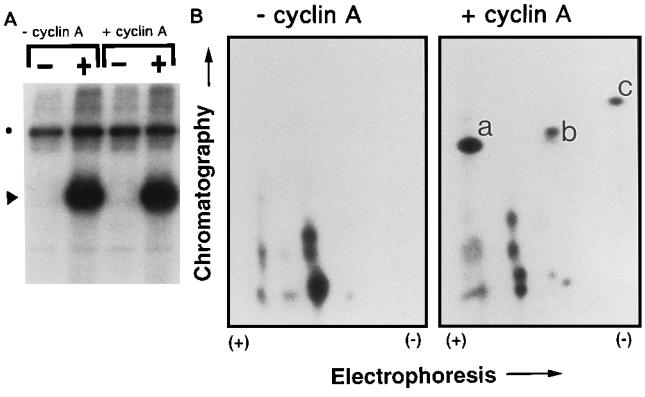

FIG. 10. Cyclin A-dependent in vitro phosphorylation of Thr-58, Ser-62, and Ser-71. (A) Autoradiogram of an SDS-polyacrylamide gel showing phosphorylated products derived from reacting purified full-length bacterial Myc protein with rabbit reticulocyte lysate programmed with or without SP6-driven cyclin A template DNA. Above each lane, + or − denotes the inclusion or exclusion of bacterial Myc protein in the kinase reaction. The phosphorylated Myc proteins were retrieved from the reaction mixture with GST-p107 prior to SDS-PAGE. The dot and arrowhead mark the positions of autophosphorylated GST-p107 (M_r, ~120,000) and Myc (lacking the HLH domain; M_r, ~62,000), respectively. (B) Maps of thermolytic Myc phosphopeptides obtained in the absence (−) or presence (+) of cyclin A. Phosphopeptides are labeled as in Fig. 7.

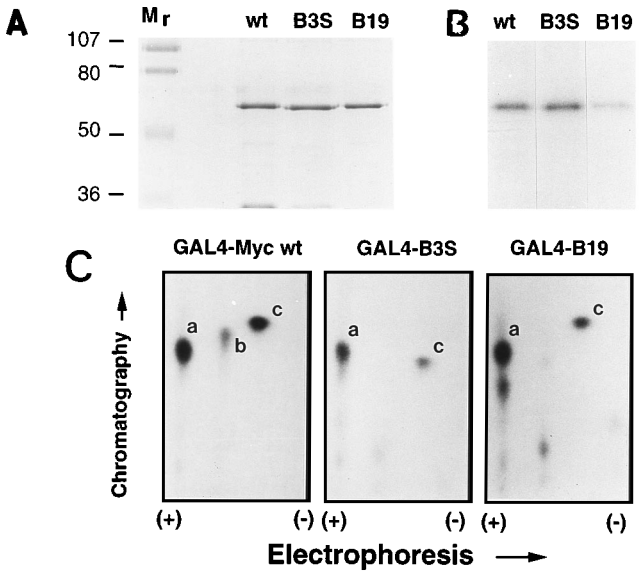

FIG. 11. Mutant GAL4-Myc chimeric proteins lack a cyclin A-dependent phosphorylation of Thr-58 in vitro. (A) Coomassie blue-stained SDS-polyacrylamide gel of purified His-tagged GAL4–wild-type Myc (wt), GAL4-B3S (B3S), and GAL4-B19 (B19) proteins. Positions (in thousands) of prestained molecular weight markers are shown on the left. (B) Autoradiogram of GAL4 chimeric proteins phosphorylated in cyclin A-programmed reticulocyte lysate separated by SDS-PAGE. Phosphorylated proteins were recovered on GST-p107 beads prior to SDS-PAGE as described for Fig. 10. (C) Thermolytic phosphopeptide maps of GAL4-Myc proteins shown in panel B. Note that only the wild-type Myc transactivation displays the thermolytic phosphopeptide b, which contains phospho-Thr-58. Phosphopeptides are labeled as in Fig. 7.

comigration experiments of in vitro-phosphorylated c-Myc peptides with in vivo-derived phosphopeptides were performed (data not shown) to verify the identities of thermolytic phosphopeptides a, b, and c. These observations suggest that Myc Ser-62 can be phosphorylated by a p107-cyclin A-CDK complex, and the ensuing phosphorylation of Thr-58 and Ser-71 may occur in a cyclin A-dependent fashion.

To correlate the transcriptional properties of wild-type or mutant GAL4-Myc chimeric proteins in the presence of p107 in vivo with their in vitro phosphorylation patterns, we produced and purified GAL4 proteins fused to c-Myc residues 1 to 252 in bacteria (Fig. 11A). These proteins were subjected to phosphorylation reactions (Fig. 11B) as described for Fig. 10. Phosphopeptide mapping of each protein (Fig. 11C) indicates that the wild-type c-Myc transactivation domain fused to GAL4 displays a cyclin A-dependent phosphorylation pattern that is reminescent of the in vivo phosphorylation pattern. The thermolytic phosphopeptide b in GAL4–wild-type Myc contains both phosphoserine and phosphothreonine (data not shown). In contrast, both the Myc-B3S and Myc-B19 mutants in identical phosphorylation reactions to the wild-type c-Myc lack the thermolytic phosphopeptide b that contains phospho-Thr-58. These results are fascinating in that mutations affecting either Pro-57 (B3S) or Pro-63 (B19) are associated with the lack of a cyclin A-dependent phosphorylation of Thr-58 in vitro. It should be noted, however, that other mutations also present in the B3S and B19 alleles (Fig. 2) may contribute to alterations in the phosphorylation of Thr-58. Our results suggest a correlation between resistance of c-Myc mutants to p107 suppression and the lack of cyclin A-dependent phosphorylation of Thr-58 in vitro.

DISCUSSION

Our results suggest that a group of lymphoma-derived mutant *MYC* alleles has increased transforming activity unassociated with an attenuated potential to induce apoptosis. This group encodes Myc proteins that resist p107-mediated suppression of Myc transactivation. These mutations cluster in *MYC* codons that encode in vivo phosphorylation sites (Thr-58 and Ser-62) in the Myc TAD. Our studies suggest that the resistance of mutant Myc proteins to p107 suppression is not due to the disruption of the physical interaction between Myc and p107. Rather, the results are compatible with the hypothesis that disruption of a p107-mediated phosphorylation of Myc may be responsible for the transforming and transactivation properties of lymphoma-derived Myc mutants.

Transforming activities of lymphoma-derived mutant *MYC* alleles. We sought to identify the biological significance of somatic mutations clustering in exon 2 of translocated *MYC* alleles frequently found in Burkitt and AIDS-related lymphomas (8, 9, 16, 60, 70). The high prevalence of these *MYC* mutations suggests that their acquisition by the tumor cells may confer either a proliferative advantage or prolonged cell survival. Therefore, we determined the transforming potential of these mutant *MYC* alleles in Rat 1a fibroblasts, which can be transformed by deregulated expression of Myc protein alone. The anchorage-independent growth of Rat 1A cells stably transfected with mutant *MYC* alleles was more robust than growth of cells expressing wild-type *MYC*. An exception was mutant B3, which contains three missense mutations in exon 2. The subcloned B3 mutation, Thr 95→Pro, which is included in the expressed full-length c-Myc protein, appears insufficient to increase transforming activity (Fig. 2 and 3). However, inclusion of all three mutations of B3 in the chimeric GAL4 protein appears to cause resistance to p107 suppression (Fig. 4b). It is unclear whether the other two B3 mutations (Gln-36→Leu and Ala-183→Val) play a role in transformation. Nevertheless, acquisition of an additional mutation (Pro-57→Phe) in a subset of tumor cells (B3S) from the same patient increases the transforming potential of c-Myc. It is notable that mutations in many of these selected *MYC* alleles are clustered around two major Myc phosphorylation sites, Thr-58 and Ser-62 (37, 51, 59). Mutation of Thr-58 has been shown by several studies to augment *MYC* transforming activity in anchorage-independent growth assays (37) as well as to transform primary cells in cooperation with an activated *RAS* gene (59). Since augmented transforming activities of mutant *MYC* alleles may result from attenuation of Myc-induced apoptosis (23, 38), we determined the extent of Myc-induced apoptosis associated with serum withdrawal and found it unaltered by enforced expression of mutant Myc compared with wild-type Myc. Thus, a selected group of lymphoma-derived Myc mutants studied herein display increased transforming activities without attenuated abilities to induced apoptosis.

Lack of a pattern of altered transactivation by Myc mutants. To determine the molecular biological consequences of mutations in *MYC* exon 2, which encodes the Myc TAD, we studied the properties of Myc-mediated transactivation in a chimeric GAL4 protein system (42). The wild-type and mutant Myc TADs were fused to the yeast GAL4 DNA-binding domain to assess the activities of these Myc TADs. The mutant Myc TADs did not display a consistent alteration in activity; i.e., some mutants were less active whereas others were more active than the wild-type Myc domain. These findings are compatible with results from several other studies. A study by Albert et al. (1) suggests that Myc transactivation is attenuated by exon 2 mutations. Further, a study by Gupta et al. (34) suggested that

mutation of either Thr-58 or Ser-62 led to decreased Myc-mediated transactivation. Neither of these studies, however, controlled for the levels of Myc proteins produced in transfected cells. The studies by Henriksson et al. (37) and Lutterbach and Hann (51) indicate that mutations at Thr-58 or Ser-62 do not result in detectable alteration of Myc-mediated transactivation. Although the basis for the differences between these studies remains to be established, our results are compatible with the observations that there is no consistent pattern of altered transactivation by Myc mutants.

Myc mutants resist suppression of transactivation by p107. Because of the lack of a pattern of altered basal transactivation capabilities of chimeric mutant Myc-GAL4 proteins, we sought to determine the effect of p107 on these mutants. Three selected lymphoma-derived Myc mutants were previously shown to resist suppression of Myc-mediated transactivation by p107 (32). Both GAL4 chimeric proteins as well as full-length mutant Myc proteins resist suppression by p107 (17a). All seven Myc mutants studied by us also resist suppression by p107 in transfection experiments. Mutations affecting Phe-115 or Phe-138 distal to Thr-58, however, do not confer resistance of Myc to p107 suppression of transactivation (69a). These observations suggest that selected lymphoma-derived mutations in *MYC* exon 2 result in mutant Myc proteins that resist suppression by p107. Since p107 suppresses growth of transfected cells, these results suggest that disruption of a functional interaction between p107 and mutant Myc may cause deregulated proliferation in the genesis of lymphomas. Future studies will be required to delineate the exact role of Myc-p107 interaction in cell cycle kinetics.

Wild-type and mutant Myc proteins bind p107 and TBP comparably. Both wild-type and mutant Myc proteins were found associated with p107 in immunoprecipitation studies with metabolically labeled lymphoma cell lines (32). These observations suggest that the altered association of p107 to mutant Myc proteins could not be detected by such methodologies or that mutations in the Myc TAD do not disrupt binding to p107. Thus, we sought to determine the mechanism by which p107 suppresses Myc-mediated transactivation activity. In vitro binding of p107 to Myc appears uninterrupted by Myc mutations. Furthermore, the interaction of all of the Myc mutants with p107 in our study was not abrogated in vivo, as determined by transfection studies using a mammalian two-hybrid system (19, 28). Our findings suggest that lymphoma-derived mutations in the Myc TAD do not disrupt the direct physical interaction of p107 and Myc.

We also examined the potential effect of mutations on the interaction of Myc with the TBP, because Myc has been shown to associate with TBP in vitro (36) and in vivo by cross-linking experiments (52). This interaction appears to involve the Myc transactivation domain. Although the significance of Myc-TBP interaction has not been thoroughly established, we sought to determine whether Myc mutations may enhance an interaction of Myc to TBP and thereby prevent the binding of p107. The Myc mutations did not dramatically augment an interaction of Myc with TBP, suggesting that this physical association is unaltered and is not responsible for resistance of Myc mutants to p107 suppression.

Phosphorylation of the Myc TAD and Myc function. Since we were unable to detect alterations in the physical association of Myc with either p107 or TBP, we sought to determine whether a functional association of p107 with Myc is perturbed by lymphoma-derived mutations. Such a putative functional interaction involving p107-mediated phosphorylation of Myc is suggested by several observations. The tumor-derived mutations considered in our studies are notably clustered around two phosphorylation sites of c-Myc, Thr-58 and Ser-62. Ser-62 is within a CDK consensus phosphorylation site and is phosphorylated by cdc2 kinase or mitogen-activated protein kinase in vitro (51). Phosphorylation of Thr-58 appears to be dependent on the prior phosphorylation of Ser-62 (37, 51, 59).

Other studies indicate that p107 binds either cyclin A or cyclin E and the associated kinases (25, 48). Such a homologous complex containing cyclin A-dependent protein kinase regulates the E2F-1 transcriptional heterodimers by phosphorylation (45).

From these observations, we hypothesize that p107-cyclin-CDK complexes phosphorylate Myc specifically at Ser-62, causing subsequent phosphorylation of Thr-58. Because mutations directly affecting Thr-58, frequently found in Burkitt lymphomas, augment Myc transforming activity, we envision that phosphorylation of Ser-62 and Thr-58 attenuates Myc function. Our in vivo phosphorylation studies suggest that a mutation flanking Thr-58 found in a Burkitt lymphoma cell line dramatically inhibits the phosphorylation of Thr-58. It is notable that mutations directly affecting Ser-62 are also observed in Burkitt lymphomas (8, 70) and that mutation of Ser-62 results in the lack of Thr-58 phosphorylation (37, 51). These observations suggest that alterations of the phosphorylation of c-Myc Ser-62 or Thr-58 may confer growth advantage to lymphoma cells. This inference is corroborated by previous in vivo experiments in which mutation at Ser-62 appears to enhance the ability of c-Myc to transform Rat 1a fibroblasts (37), although its ability to transform primary fibroblasts in cooperation with an activated *RAS* gene may be attenuated (59).

Implications of in vitro phosphorylation of Myc by a p107-cyclin A-CDK complex. We also sought to determine whether a p107-cyclin A-CDK complex phosphorylates the Myc transactivation domain. Using an affinity-purified cyclin A-CDK complex associated with GST-p107 and a Myc substrate, we observe that Ser-62 is specifically phosphorylated. In addition, we found that Myc protein is phosphorylated in vitro at Thr-58, Ser-62, and Ser-71 in a cyclin A-dependent fashion, using reticulocyte lysate. Phosphorylation of Myc by unprogrammed reticulocyte lysate did not result in modifications of these residues. All three of these residues are also phosphorylated in vivo, suggesting that cyclin A-CDK may mediate a priming phosphorylation reaction at Ser-62. Such a priming reaction presumably allows other kinases to modify Thr-58 and thereby inactivate Myc function, perhaps by disrupting its interaction with TBP-associated factors (68). This model does not account for results from two studies reporting different transactivation properties of Myc altered at either Thr-58 or Ser-62 (34, 51). Thus, studies designed to specifically address these issues will be necessary to test further our proposed model.

Although our results are compatible with the hypothesis that p107 regulates Myc function through phosphorylation, a number of questions must be considered. Why would a p107-cyclin-CDK complex inactivate a protein (c-Myc) that promotes cellular proliferation? From the observations that Myc expression augments cyclin A expression (38, 40) and presumably allows cells to enter and traverse through S phase, we speculate that a feedback mechanism involving cyclin A to attenuate Myc function during or at the end of S phase would be compatible with this view. The attenuation of Myc function at the end of S phase would lead to a normal and timely down-modulation of cyclin A expression. Analogously, cyclin A kinase associates with E2F-1 and phosphorylates the partner protein DP-1 to inactivate E2F-1-dependent transactivation in late S phase (45). It is speculated that the inactivation of E2F-1 would lead to the down-modulation of E2F-1-dependent S-phase-specific gene expression. Although mutation of Thr-58 augments Myc

transforming activity, why do mutations of Thr-58 and Ser-62 not augment Myc transactivation potential in a consistent fashion? This issue remains to be resolved; however, we expect that carefully designed studies to examine cell cycle-specific events and the use of elutriate cells will shed light on this matter. Considered with these limitations, the hypothesis that we proposed provides a testable model for future studies and suggests a mechanism of interaction between a growth-suppressing protein, p107, and the product of the proto-oncogene *MYC*.

ACKNOWLEDGMENTS

We thank E. Fearon, W. Kaelin, and D. Wechsler for suggestions and M. Ewen, J. Gralla, D. Hawley, R. Wisdom, and W. Kaelin for plasmids. We thank R. Bernards and R. Dalla-Favera for sharing information prior to publication.

This work was in part supported by the Wilbur-Rogers Foundation (C.V.D. and A.T.H.) and NIH grants CA57341 (C.V.D.), CA51497 (C.V.D.), CA47399 (S.R.H.), and CA46799 (S.R.H.). B.C.L. is supported by a Howard Hughes predoctoral fellowship and NIH Human Genetics training grant T32GM07814. C.V.D. is a Leukemia Society of America Scholar.

REFERENCES

1. **Albert, T., B. Urlbauer, F. Kohlhuber, D. Eick, and B. Hammersen.** 1994. Ongoing mutations in the N-terminal domain of c-Myc affect transactivation in Burkitt's lymphoma cell lines. Oncogene **9:**759–763.
2. **Amati, B., M. W. Brooks, N. Levy, T. D. Littlewood, G. I. Evan, and H. Land.** 1993. Oncogenic activity of the c-Myc protein requires dimerization with Max. Cell **72:**233–245.
3. **Amati, B., S. Dalton, M. W. Brooks, T. D. Littlewood, G. I. Evan, and H. Land.** 1992. Transcriptional activation by the human c-Myc oncoprotein in yeast requires interaction with Max. Nature (London) **359:**423–426.
4. **Barrett, J., M. J. Birrer, G. J. Kato, H. Dosaka-Akita, and C. V. Dang.** 1992. Activation domains of L-Myc and c-Myc determine their transforming potencies in rat embryo cells. Mol. Cell. Biol. **12:**3130–3137.
5. **Beijersbergen, R. L., E. M. Hijmans, L. Zhu, and R. Bernards.** 1994. Interaction of c-Myc with the pRb-related protein p107 results in inhibition of c-Myc mediated transactivation. EMBO J. **13:**4080–4086.
6. **Bello-Fernandez, C., G. Packham, and J. L. Cleveland.** 1993. The ornithine decarboxylase gene is a transcriptional target of c-Myc. Proc. Natl. Acad. Sci. USA **90:**7804–7808.
7. **Berberich, S. J., and M. D. Cole.** 1992. Casein kinase II inhibits the DNA-binding activity of Max homodimers but not Myc/Max heterodimers. Genes Dev. **6:**166–176.
8. **Bhatia, K., K. Huppi, G. Spangler, D. Siwarski, R. Iyer, and I. Magrath.** 1993. Point mutations in the c-Myc transactivation domain are common in Burkitt's lymphoma and mouse plasmacytoma. Nat. Genet. **5:**56–61.
9. **Bhatia, K., G. Spangler, G. Gaidano, N. Hamdy, R. DallaFavera, and I. Magrath.** 1994. Mutations in the coding region of c-myc occur frequently in acquired immunodeficiency syndrome-associated lymphomas. Blood **84:**883–888.
10. **Blackwell, T. K., J. Huang, A. Ma, L. Kretzner, F. W. Alt, R. N. Eisenman, and H. Weintraub.** 1993. Binding of Myc proteins to canonical and noncanonical DNA sequences. Mol. Cell. Biol. **13:**5216–5224.
11. **Blackwell, T. K., L. Kretzner, E. M. Blackwood, R. N. Eisenman, and H. Weintraub.** 1990. Sequence-specific DNA binding by the c-Myc protein. Science **250:**1149–1151.
12. **Blackwood, E. M., and R. N. Eisenman.** 1991. Max: a helix-loop-helix zipper protein that forms a sequence-specific DNA-binding complex with Myc. Science **251:**1211–1217.
13. **Blackwood, E. M., L. Kretzner, and R. N. Eisenman.** 1992. Myc and Max function as a nucleoprotein complex. Curr. Opin. Genet. Dev. **2:**227–235.
14. **Boyle, W. J., P. van der Greer, and T. Hunter.** 1991. Phosphopeptide mapping and phosphopeptide analysis by two-dimensional separation on thin-layer cellulose plates. Methods Enzymol. **201:**110–149.
15. **Chang, C., and J. D. Gralla.** 1993. Properties of initiator-associated transcription mediated by GAL4-VP16. Mol. Cell. Biol. **13:**7469–7475.

15a. **Chou, T. Y.** Unpublished data.

16. **Clark, H. M., T. Yano, T. Otsuki, E. S. Jaffe, D. Shibata, and M. Raffeld.** 1994. Mutations in the coding region of c-myc in AIDS-associated and other aggressive lymphomas. Cancer Res. **54:**3383–3386.
17. **Cole, M. D.** 1991. Myc meets its max. Cell **65:**715–716.

17a. **Dalla-Favera, R.** Personal communication.

18. **Dang, C. V.** 1991. c-Myc oncoprotein function. Biochim. Biophys. Acta **1072:**103–113.
19. **Dang, C. V., J. Barrett, M. Villa-Garcia, L. M. S. Resar, G. J. Kato, and E. R. Fearon.** 1991. Intracellular leucine zipper interactions suggest c-Myc hetero-oligomerization. Mol. Cell. Biol. **11:**954–962.
20. **Dang, C. V., M. McGuire, M. Buckmire, and W. M. F. Lee.** 1989. Involvement of the 'leucine zipper' region in the oligomerization and transforming activity of human c-myc protein. Nature (London) **337:**664–666.
21. **DePinho, R. A., N. Schreiber-Agus, and F. W. Alt.** 1991. *myc* family oncogenes in the development of normal and neoplastic cells. Adv. Cancer Res. **57:**1–46.

21a. **Dolde, C., and C. Dang.** Unpublished data.

22. **Dyson, N., K. Buchkovich, P. Whyte, and E. Harlow.** 1989. The cellular 107K protein that binds to adenovirus E1A also associates with the large T antigens of SV40 and JC virus. Cell **58:**249–255.
23. **Evan, G., A. Wyllie, C. Gilbert, T. Littlewood, H. Land, M. Brooks, C. Waters, L. Penn, and D. Hancock.** 1992. Induction of apoptosis in fibroblasts by c-Myc protein. Cell **69:**119–128.
24. **Ewen, M., Y. Xing, J. Lawrence, and D. Livingston.** 1991. Molecular cloning, chromosomal mapping, and expression of the cDNA for p107, a retinoblastoma gene product-related protein. Cell **66:**1155–1164.
25. **Ewen, M. E., B. Faha, E. Harlow, and D. M. Livingston.** 1992. Interaction of p107 with cyclin A independent of complex formation with viral oncoproteins. Science **255:**85–87.
26. **Ewen, M. E., J. W. Ludlow, E. Marsilio, J. A. DeCaprio, R. C. Millikan, S. H. Cheng, E. Paucha, and D. M. Livingston.** 1989. An N-terminal transformation-governing sequence of SV40 large T antigen contributes to the binding of both p110Rb and a second cellular protein, p120. Cell **58:**257–267.
27. **Faha, B., M. E. Ewen, L. H. Tsai, D. M. Livingston, and E. Harlow.** 1992. Interaction between human cyclin A and adenovirus E1A-associated p107 protein. Science **255:**87–90.
28. **Fearon, E., T. Finkel, M. Gillison, S. Kennedy, J. Casella, G. Tomaselli, J. Morrow, and C. Dang.** 1992. Karyoplasmic interaction selection strategy: a general strategy to detect protein-protein interactions in mammalian cells. Proc. Natl. Acad. Sci. USA **89:**7958–7962.
29. **Ferre-D'Amare, A., G. Prendergast, E. Ziff, and S. Burley.** 1993. Recognition by Max of its cognate DNA through a dimeric b/HLH/Z domain. Nature (London) **363:**38–45.
30. **Flemington, E. K., S. H. Speck, and W. Kaelin, Jr.** 1993. E2F-1-mediated transactivation is inhibited by complex formation with the retinoblastoma susceptibility gene product. Proc. Natl. Acad. Sci. USA **90:**6914–6918.
31. **Gavrieli, Y., Y. Sherman, and S. A. Ben-Sasson.** 1992. Identification of programmed cell death in situ via specific labeling of nuclear DNA fragmentation. J. Cell Biol. **119:**493–501.
32. **Gu, W., K. Bhatia, I. T. Magrath, C. V. Dang, and R. Dalla-Favera.** 1994. Binding and suppression of the myc transcriptional activation domain by p107. Science **264:**251–254.
33. **Gu, W., K. Cechova, V. Tassi, and R. Dalla-Favera.** 1993. Opposite regulation of gene transcription and cell proliferation by c-Myc and Max. Proc. Natl. Acad. Sci. USA **90:**2935–2939.
34. **Gupta, S., A. Seth, and R. Davis.** 1993. Transactivation of gene expression by Myc is inhibited by mutation at the phosphorylation sites Thr-58 and Ser-62. Proc. Natl. Acad. Sci. USA **90:**3216–3220.
35. **Harlow, E., P. Whyte, B. Franza, Jr., and C. Schley.** 1986. Association of adenovirus early-region 1A proteins with cellular polypeptides. Mol. Cell. Biol. **6:**1579–1589.
36. **Hateboer, G., H. T. M. Timmers, A. K. Rustgi, M. Billaud, L. J. van't Veer, and R. Bernards.** 1993. TATA-binding protein and the retinoblastoma gene product bind to overlapping epitopes on c-Myc and adenovirus E1A protein. Proc. Natl. Acad. Sci. USA **90:**8489–8493.
37. **Henriksson, M., A. Bakardjiev, G. Klein, and B. Luscher.** 1993. Phosphorylation sites mapping in the N-terminal domain of c-*myc* modulate its transforming potential. Oncogene **8:**3199–3209.
38. **Hoang, A. T., K. J. Cohen, J. F. Barrett, D. A. Bergstrom, and C. V. Dang.** 1994. Participation of cyclin A in myc-induced apoptosis. Proc. Natl. Acad. Sci. USA **91:**6875–6879.

38a. **Hoang, A. T., and C. V. Dang.** Unpublished data.

39. **Hoang, A. T., W. Wang, and J. D. Gralla.** 1992. The replication activation potential of selected RNA polymerase II promoter elements at the simian virus 40 origin. Mol. Cell. Biol. **12:**3087–3093.
40. **Jansen-Durr, P., A. Meichle, P. Steiner, M. Pagano, D. Finke, J. Botz, J. Wessbecher, G. Draetta, and M. Eilers.** 1993. Differential modulation of cyclin gene expression by MYC. Proc. Natl. Acad. Sci. USA **90:**3685–3689.
41. **Kaelin, W., Jr., W. Krek, W. R. Sellers, et al.** 1992. Expression cloning of a cDNA encoding a retinoblastoma-binding protein with E2F-like properties. Cell **70:**351–364.
42. **Kato, G. J., J. Barrett, M. Villa-Garcia, and C. V. Dang.** 1990. An amino terminal c-Myc domain required for neoplastic transformation activates transcription. Mol. Cell. Biol. **10:**5914–5920.
43. **Kato, G. J., and C. V. Dang.** 1992. Function of the c-Myc oncoprotein. FASEB J. **6:**3065–3072.
44. **Kato, G. J., W. M. F. Lee, L. Chen, and C. V. Dang.** 1992. Max: functional domains and interaction with c-Myc. Genes Dev. **6:**81–92.
45. **Krek, W., M. E. Ewen, S. Shirodkar, Z. Arany, W. G. Kaelin, and D. M. Livingston.** 1994. Negative regulation of the growth-promoting transcription factor E2F-1 by a stably bound cyclin A-dependent protein kinase. Cell **78:**161–172.
46. **Kretzner, L., E. M. Blackwood, and R. N. Eisenman.** 1992. Myc and Max

proteins possess distinct transcriptional activities. Nature (London) **359:**426–429.
47. **Laemmli, U. K.** 1970. Cleavage of structural proteins during the assembly of the head of bacteriophage T4. Nature (London) **227:**680–685.
48. **Lees, E., B. Faha, V. Dulic, S. Reed, and E. Harlow.** 1992. Cyclin E/cdk2 and cyclin A/cdk2 kinases associate with p107 and E2F in a temporally distinct manner. Genes Dev. **6:**1874–1885.
49. **Li, L.-H., C. Nerlov, G. Prendergast, D. MacGregor, and E. B. Ziff.** 1994. c-Myc represses transcription in vivo by a novel mechanism dependent on the initiator element and Myc box II. EMBO J. **13:**4070–4079.
50. **Littlewood, T. D., B. Amati, H. Land, and G. I. Evan.** 1992. Max and c-Myc/Max DNA-binding activities in cell extracts. Oncogene **7:**1783–1792.
51. **Lutterbach, B., and S. R. Hann.** 1994. Hierarchical phosphorylation at N-terminal transformation-sensitive sites in c-Myc protein is regulated by mitogens and in mitosis. Mol. Cell. Biol. **14:**5510–5522.
52. **Maheswaran, S., H. Lee, and G. Sonenshein.** 1994. Intracellular association of the protein product of the c-*myc* oncogene with the TATA-binding protein. Mol. Cell. Biol. **14:**1147–1152.
53. **Mermod, N., E. A. O'Neill, T. J. Kelly, and R. Tjian.** 1989. The proline-rich transcriptional activator of CTF/NF1 is distinct from the replication and DNA binding domain. Cell **58:**741–753.
54. **Papas, T., and J. Lautenberg.** 1985. Sequence curiosity in v-*myc* oncogene. Nature (London) **318:**237.
55. **Philipp, A., A. Schneider, I. Väsrik, K. Finke, Y. Xiong, D. Beach, K. Alitalo, and M. Eilers.** 1994. Repression of cyclin D1: a novel function of MYC. Mol. Cell. Biol. **14:**4032–4043.
56. **Pines, J., and T. Hunter.** 1990. Human cyclin A is adenovirus E1A-associated protein p60 and behaves differently from cyclin B. Nature (London) **346:**760–763.
57. **Prendergast, G. C., and E. B. Ziff.** 1991. Methylation-sensitive sequence-specific binding by the c-Myc basic region. Science **251:**186–188.
58. **Prendergast, G. C., and E. B. Ziff.** 1992. A new bind for Myc. Trends Genet. **8:**91–96.
59. **Pulverer, B. J., C. Fisher, K. Vousden, T. Littlewood, G. Evan, and J. R. Woodgett.** 1994. Site-specific modulation of c-Myc cotransformation by residues phosphorylated *in vivo*. Oncogene **9:**59–70.
60. **Rabbitts, T., P. Hamlyn, and R. Baer.** 1983. Altered nucleotide sequences of a translocated c-*myc* gene in Burkitt lymphoma. Nature (London) **306:**760–765.
61. **Resar, L. M., C. Dolde, J. F. Barrett, and C. V. Dang.** 1993. B-Myc inhibits neoplastic transformation and transcriptional activation by c-Myc. Mol. Cell. Biol. **13:**1130–1136.
62. **Roy, A. L., C. Carruthers, T. Gutjahr, and R. G. Roeder.** 1993. Direct role for Myc in transcription initiation mediated by interactions with TFII-I. Nature (London) **365:**359–361.
63. **Roy, A. L., M. Meisterernst, P. Pogenec, and R. G. Roeder.** 1991. Cooperative interaction of an initiator-binding transcription initiation factor and the helix-loop-helix activator USF. Nature (London) **354:**245–248.
64. **Seth, A., S. Gupta, and R. J. Davis.** 1993. Cell cycle regulation of the c-Myc transcriptional activation domain. Mol. Cell. Biol. **13:**4125–4136.
65. **Shirodkar, S., M. Ewen, J. A. DeCaprio, J. Morgan, D. M. Livingston, and T. Chittenden.** 1992. The transcription factor E2F interacts with the retinoblastoma product and a p107-cyclin A complex in a cell cycle-regulated manner. Cell **68:**157–166.
66. **Starr, D. B., and D. K. Hawley.** 1991. TFIID binds in the minor groove of the TATA box. Cell **67:**1231–1240.
67. **Stone, J., T. de Lange, G. Ramsay, E. Jokobovits, J. M. Bishop, H. E. Varmus, and W. M. F. Lee.** 1987. Definition of regions in human c-*myc* that are involved in transformation and nuclear localization. Mol. Cell. Biol. **7:**1697–1709.
68. **Tjian, R., and T. Maniatis.** 1994. Transcriptional activation: a complex puzzle with few easy pieces. Cell **77:**5–8.
69. **Wenzel, A., C. Cziepluch, U. Hamann, J. Schürmann, and M. Schwab.** 1991. The N-Myc oncoprotein is associated in vivo with the phosphoprotein Max (p20/22) in human neuroblastoma cells. EMBO J. **10:**3703–3712.
69a. **Yano, T., and H. Clark.** Unpublished data.
70. **Yano, T., C. Sander, H. Clark, M. Dolezal, E. Jaffe, and M. Raffeld.** 1993. Clustered mutations in the second exon of the MYC gene in sporadic Burkitt's lymphoma. Oncogene **8:**2741–2748.
71. **Yee, S. P., and P. E. Branton.** 1985. Detection of cellular proteins associated with human adenovirus type 5 early region 1A polypeptides. Virology **147:**142–153.
72. **Zhu, L., S. van den Heuvel, K. Helin, A. Fattaey, M. Ewen, D. Livingston, N. Dyson, and E. Harlow.** 1993. Inhibition of cell proliferation by p107, a relative of the retinoblastoma protein. Genes Dev. **7:**1111–1125.